GLIA 25:190–198 (1999)

Early Microglial Response in Experimental Thiamine Deficiency: An Immunohistochemical Analysis

KATHRYN G. TODD AND ROGER F. BUTTERWORTH*
Neuroscience Research Unit, Hôpital St-Luc (University of Montreal), Montreal, Canada

KEY WORDS thiamine deficiency; ED-1 immunohistochemistry; neuronal cell death; Wernicke Encephalopathy; microglia/macrophage

ABSTRACT Early glial changes have consistently been reported in experimental thiamine deficiency (TD) (Tellez and Terry, Am. J. Pathol. 52:777–794, 1968.) and in Wernicke Encephalopathy in humans (Victor et al., F.A. Davis Co., Philadelphia, 1989.). However, the precise nature of these changes and their relationship to the phenomenon of selective neuronal cell loss in TD has not been elucidated. In the present studies, antibodies against GFAP and ED1 were used to evaluate astrocytic and microglial/macrophagic changes respectively in adjacent sections of the brains of thiamine-deficient rats at various stages (n = 6 per stage) during the progression of encephalopathy. Additionally, the integrity of the blood–brain barrier at the same stages was assessed using IgG immunohistochemistry. Counts of immuno-positive cells revealed significant increases of ED1-immunostaining in the inferior olive, medial geniculate nucleus, and medial thalamic nuclei on day 8 of the treatment paradigm, prior to any evidence of increased IgG immunostaining or significant neuronal cell loss. ED1 immunostaining increased over time, resulting in intense staining by the loss of righting reflex stage (day 13–15). Focal increases of IgG-immunoreactivity in inferior olive, medial dorsal thalamus, and medial geniculate nucleus were observed on day 10, followed by increased GFAP-immunostaining consistent with reactive gliosis. Early microglial activation leading to the release of cytotoxic substances including reactive oxygen species, glutamate and cytokines appears to be the initial cellular response to TD and could be responsible for the focal neuronal loss characteristic of this disorder. *GLIA 25:190–198, 1999.*

INTRODUCTION

In the central nervous system (CNS), the reaction of tissue to focal damage, such as that induced by a local ischemic lesion or neurotoxin injection, is characterized by proliferation of reactive astroglia and microglia/macrophages and infiltration of blood-borne phagocytes. It was reported that activated microglia were the predominant glial cell type in early CNS injury and as such likely play a key role in the evolution of cellular constinuents in area of subsequent neuronal loss (Myers et al., 1991).

Severe thiamine deficiency (TD), in humans and animal models, results in highly selective focal lesions in the CNS. Neuropathologic studies in animals with experimentally induced TD have consistently shown that the initial cellular insult involves glial cells rather than neurons (Collins, 1967; Robertson et al., 1968; Tellez and Terry, 1968; Watanabe and Kanabe, 1978; Aikawa et al., 1984). Alterations of both astrocytes and microglia/macrophages were described in these early reports. The majority of these studies focussed on morphological changes such as soma swelling and swelling and vacuolation of astroglia end-feet (Collins, 1967; Watanabe and Kanabe, 1978).

Contract grant sponsor: Medical Research Council of Canada; Contract grant number: MT9156.

*Correspondence to: Dr. Roger F. Butterworth, Neuroscience Research Unit, Andre-Viallet Clinical Research Centre, Hôpital Saint-Luc, 1058 St. Denis Street, Montreal, Quebec, H2X 3J4, Canada.

Received 1 December 1997; Accepted 15 July 1998

However, the temporal sequence of astrocytic vs. microglial/macrophagic changes in relation to known alterations in permeability of the blood-brain barrier and neuronal cell loss due to TD has not been established. Therefore, the purpose of the present studies, was to investigate astrocytic and microglial changes at different stages of evolution of TD and to relate these changes to alterations in blood–brain barrier permeability and to neuronal cell loss.

To assess the regional and temporal distribution and relative densities of astrocytes, antibodies against glial fibrillary acidic protein GFAP were used as immunohistochemical markers. For identification of activated microglial/macrophages, ED1 antibodies were employed. ED1 recognizes an as yet uncharacterized cytoplasmic antigen in adult CNS, and labels perivascular as well as activated microglia/macrophages (Graeber et al., 1990; Gehrmann and Kreutzberg, 1993; Aihara et al., 1995). Blood–brain barrier (BBB) permeability was assessed by using immunoglobulin G (IgG) one-step immunohistochemistry. This method of measuring BBB integrity was selected as it has been used previously in experimental TD and was shown to be sensitive to early changes in the BBB that occurred prior to neuronal cell death in this condition (Calingasan et al., 1995).

MATERIALS AND METHODS

Treatment Groups

Male Sprague-Dawley rats weighing 200–225 g were used for the experiments described. Animals were housed individually in wire mesh cages under constant conditions of temperature and humidity, and with 12 h light/dark cycles. Upon arrival at our animal housing facilities, rats were allowed to acclimatize for three days with ad libitum access to food and water. At the initiation of the experiments, the animals were randomly assigned to either pyrithiamine-induced TD groups or pair-fed controls. All animal procedures conformed to guidelines of the Animal Ethics Committee of Hôpital St-Luc and the University of Montreal.

Animals in the TD group were fed a thiamine deficient diet (ICN, Nutritional Biochemical, Cleveland, OH) and administered daily pyrithiamine hydrobromide at a dose of 50 μg/100 g body weight, subcutaneously (sc). Pair-fed control (CON) animals were fed the same thiamine deficient diet pair-fed to equal food consumption to that of rats in the TD group. In addition, these rats received daily sc thiamine injections in a dose of 10 μg/100 g body weight. Commencing on day 3 of the treatment protocol, groups of six TD and four CON animals were sacrificed each day up to and including day 15 by which time the final group of six TD animals had all exhibited loss of righting reflexes. The righting reflex was considered absent when the animal was no longer able to right itself when placed on its back. Any rats showing seizure activity were eliminated from the protocol. The animals were sacrificed by decapitation, the brains removed, flash frozen in isopentane on dry ice, and stored at −80°C until sectioning on a microtome cryostat.

Serial sagittal slices 20 μm thick from 0.9, 1.4, 1.9, 2.4, and 3.4 mm lateral according to the rat brain atlas of Paxinos and Watson (1982) were used in the studies. The areas included for immohistological and histological assessment and classically considered to be vulnerable to TD were thalamic nuclei (including the medial and lateral geniculate nuclei); mammillary bodies; inferior colliculus; and inferior olive, medial, and lateral vestibular nuclei; those considered not vulnerable to TD were the caudate nucleus and frontal motor cortex (Victor et al., 1989; Zhang et al., 1995).

Immunohistochemistry

ED1 immunostaining was performed using silver enhancement according to the protocol of Jackson ImmunoResearch Laboratories Inc (West Grove, PA). Briefly, slides were allowed to warm to room temperature for 1 h and then incubated with phosphate-buffered saline (PBS) containing 0.05% Tween 20 (PBS-Tw) and 4% normal mouse serum for 20 min at room temperature. Sections were then incubated with monoclonal anti-mouse ED1 (1:500, Serotec, Ltd., Raleigh, NC) for 24 h at 4°C in a humidified chamber followed by three washes of 5 min with PBS-Tw. Pilot studies of varying primary antibody concentrations showed that this dilution resulted in very low to absent staining in control rat brain, thus making any increases in immunostaining more obvious. The secondary 4 nM (LM grade) colloidal gold-antibody was then applied at a dilution of 1:50 and incubated for 1 h in the humidified chamber. After four 5 min washes in PBS-Tw and two washes of 5 min in PBS without Tween-20, sections were postfixed in 1% glutaraldehyde in PBS for 10 min. Three more washes for 5 min with PBS were followed by five changes of distilled water for a total of 10 min. The silver enhancement reaction was carried out by initially placing the slides for 5 min in citrate buffer containing hydroquinone (pH 3.8). Slides were then transferred to a developer containing equal volumes of citrate buffer and a silver acetate solution for 10–15 min. After a quick rinse in distilled water, the slides were placed in a commercial photographic fixative for 2 min, rinsed with tap water for at least 5 min, dehydrated in graded alcohols, cleared in xylenes, and mounted in Permount.

For GFAP immunostaining, frozen 20 μm sections were allowed to warm to room temperature and incubated for 20 min at room temperature in alcohol/H_2O_2 (99:1) to quench endogenous peroxidase activity. Sections were then rinsed in Tris buffer (pH 7.4) and incubated in normal horse serum (1:10 in Tris) for 30 min to block nonspecific background. Sections were incubated with polyclonal rabbit anti-cow GFAP (Dako, Ltd., Mississauga, Ontario, Canada; 1:1,000) in a humidified chamber for 2 h. After three rinses for a total of 15 min in Tris buffer, the secondary antibody (anti-

rabbit IgG, 1:200 for GFAP) was applied for 1 hr. After 3 rinses (5 min each) in Tris buffer, the avidin-biotin complex (Vector Laboratories, Burlingame, CA; 1:100) was applied and the reaction product visualized using 3,3′diaminobenzidine tetrahydrochloride-hydrogen peroxide (DAB). Sections were dehydrated in graded alcohols, cleared in xylenes and mounted in Permount.

IgG immunohistochemistry was carried out as described by Calingasan et al. (1995) with minor modifications. Briefly, sections were incubated for 20 min with 0.1% H_2O_2 and 1% normal goat serum followed by three rinses for a total of 15 min in PBS containing 0.3% Triton-X 100 (PBS-TX, pH 7.4). Anti-rabbit IgG secondary antibody diluted 500 times in PBS was applied to the sections for 1 h, followed by application of the avidin-biotin complex (1:100) and the reaction product visualized with DAB. Negative control slides for all antibodies were treated in an identical manner except they were incubated without primary antibodies.

Adjacent sections to those used for immunohistochemistry were stained with standard histological protocols using cresyl violet for neuronal cell counting. ED1 and GFAP-immunoreactive cells and cresyl violet stained neurons were counted and averaged in at least two fields of 0.025 mm^2/image field for smaller nuclei, and at least six fields for larger nuclei, resulting in approximately 75% of the total nuclei being sampled.

Anatomical borders based on the atlas of Paxinos and Watson (1982) were used to define the various nuclei. Clusters of ED1-positive cells were counted as one cell, thus a conservative counting strategy was employed. Individual cells positively stained for GFAP were easily identified and quantified. Criteria for neuronal count inclusion was based upon nuclear size and the presence of a nucleolus as described previously (Todd and Butterworth, 1998). IgG immunolabelling was graded as either absent (−), mild (+, occasional IgG labelling outside a vessel wall), moderate (++, 50–75% of the region showing intense labelling), or intense (+++, more than 75% of the region showing intense labelling). Evaluation of all sections were carried out by an investigator unaware of the treatment groups.

Statistical Analysis

Two-way analysis of variance (ANOVA, InStat computer program), with treatment as one factor and day as the other, was used to compare the number of positively stained cells after ED1 and GFAP-immunostaining and after cresyl violet staining. Where significant main effects were achieved, post hoc Newman Keuls multiple comparisons were run to ascertain significantly different groups. For albumin immunostaining, non parametric Kruskal-Wallis Tests were run to identify significantly different groups. A probability of $P < 0.05$ was chosen to represent statistical significance.

RESULTS

Behavioral Observations

On day 10, TD animals developed anorexia, and significant weight loss was observed in these animals by days 11–14. Equivalent weight loss was observed in the control animals pair fed to the TD animals (data not shown). TD animals showed neurological symptoms including ataxia, exophthalmos, and increased startle reflex commencing on day 11. By day 12, individual animals started to exhibit severe ataxia and ultimately lost their righting reflex. Pair-fed control animals showed no signs of neurological impairment.

Histology

Histopathological evaluation of sections from animals sacrificed from days 3–10 revealed no significant neuronal loss in the areas considered vulnerable to thiamine deficiency. Figure 1 displays representative photomicrographs obtained from the medial geniculate nucleus after cresyl violet staining in CON rats (a), and TD rats at 8 days (b), and at loss of righting reflex (c). Gross inspection did however reveal occasional pinpoint haemorrhagic lesions in individual animals after 10 days of TD in the inferior olive, lateral vestibular nucleus, and medial geniculate nucleus. On day 12, moderate neuronal loss was apparent (33% loss) in some thalamic nuclei. In all animals sacrificed at the loss of righting reflex stage, histological examination revealed evidence of more marked neuronal loss, pallor of the neuropil, necrosis, and marked gliosis in thalamic nuclei, inferior colliculus, inferior olive, medial ventricular nucleus, and mammillary bodies. No evidence of neuronal loss or gliosis was observed in the striatum or frontal motor cortex.

Immunohistochemistry

Alterations of ED1 and GFAP-immunostaining were regionally and temporally distinct. Starting on day 8 of treatment, ED1 immunostaining was significantly increased in the mammillary bodies (lateral), inferior colliculus, inferior olive, medial and lateral vestibular nuclei, and thalamus of TD animals compared to control animals. On day 7, sections obtained from three TD animals showed increased ED1 immunostaining confined to the periventricular nucleus of the thalamus (data not shown). These cells appeared rod-like, with short, stout processes. ED1 immunostaining in the periventricular nucleus and all other vulnerable regions increased progressively over the subsequent days and was maximal at day 12. Figure 2 displays representative photomicrographs of ED1 immunostaining in the medical geniculate nucleus of CON (a) and TD rats on day 8 (b), and at the loss of righting reflex stage (c). A similar staining pattern was obtained in other areas considered vulnerable to TD including other thalamic

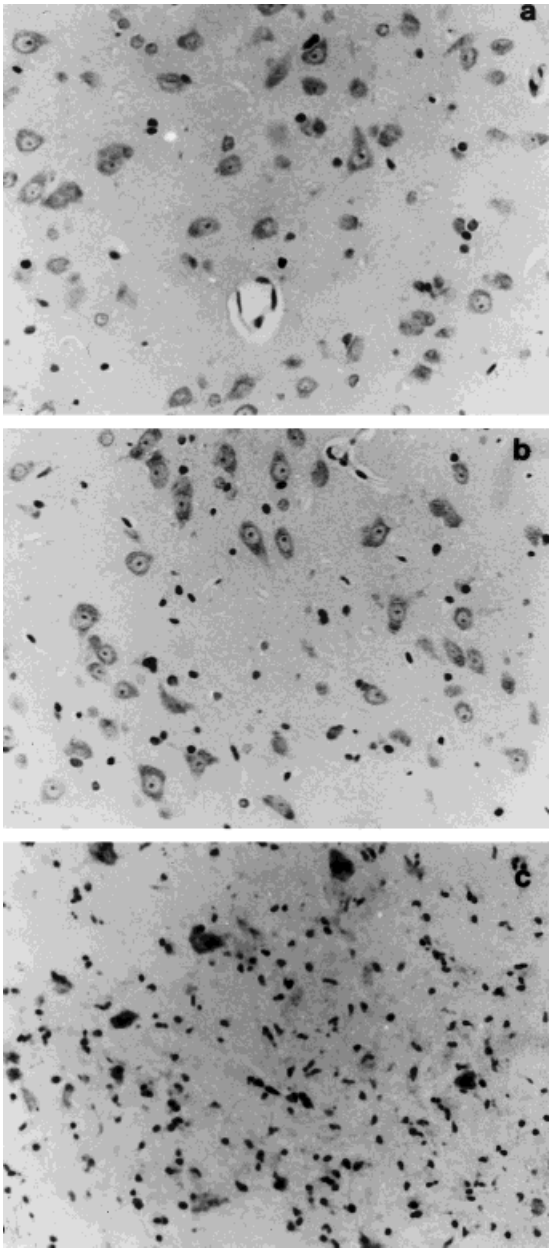

Fig. 1. Representative photomicrographs after cresyl violet staining for identification of neurons in the medial geniculate nucleus. **a:** From a control rat. **b,c:** sections from TD rats sacrificed after 8 days and at the loss of righting reflex stage, respectively (all ×250). There is an increased number of glial cells without apparent loss of neurons after 8 days of TD compared to the control animal. At the loss of righting reflex stage, the region is almost devoid of neurons, and shows extensive glial proliferation.

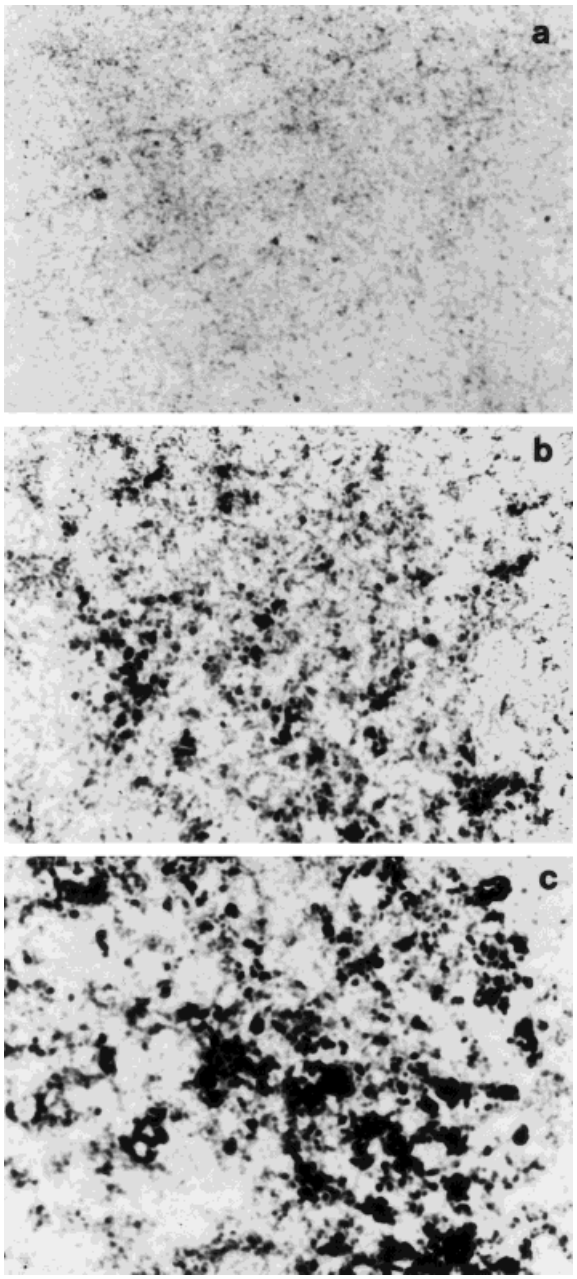

Fig. 2. Representative photomicrographs of ED1 immunostaining in the medial geniculate nucleus. **a:** From a control rat. **b,c:** Sections from TD rats sacrificed after 8 days and at the loss of righting reflex stage, respectively (all ×250). Positive ED1 immunostaining is observed after 8 days of treatment and the number of immuno-positive cells is significantly increased by the loss of righting reflex stage (c).

nuclei, inferior colliculus, mamillary bodies, and the medial vestibular nuclei. On day 12, the majority of ED1-positive cells appeared spherical, with round cell bodies, and, if present, short, stout processes (i.e., these cells lacked ramified-type processes).

In contrast, increased GFAP immunostaining was not observed until day 11 of the TD treatment protocol. GFAP immunostaining was initially observed in the medial thalamic, inferior olivary, and medial and lateral vestibular nuclei extending, at later stages, to the lateral thalamic nuclei and inferior colliculus. These cells typically had larger cell bodies with thickened stellar processes compared to those of control rats. Representative photomicrographs from the medial geniculate nucleus of the thalamus from CON (a) and TD animals at 8 days (b), and at the loss of righting reflex stage (c) are displayed in Figure 3.

Examination of sections from TD animals also revealed focal increases of IgG immunostaining in vulner-

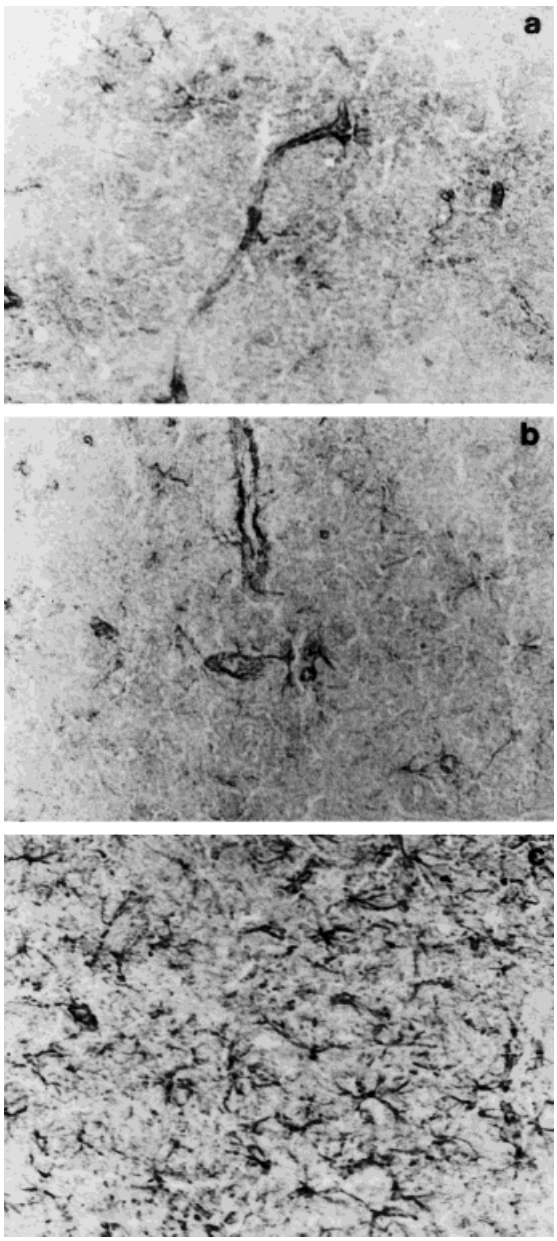

Fig. 3. Representative photomicrographs of GFAP immunostaining in the medial geniculate nucleus. **a:** From a control rat. **b,c:** Sections from TD rats sacrificed after 8 days and at the loss of righting reflex stage respectively (all ×250). Unlike the ED1 immunostaining, no increase in GFAP immunostaining was observed at day 8 of TD (b) as compared with controls. GFAP-positive astrocytes are observed throughout the field at the loss of righting reflex stage (c).

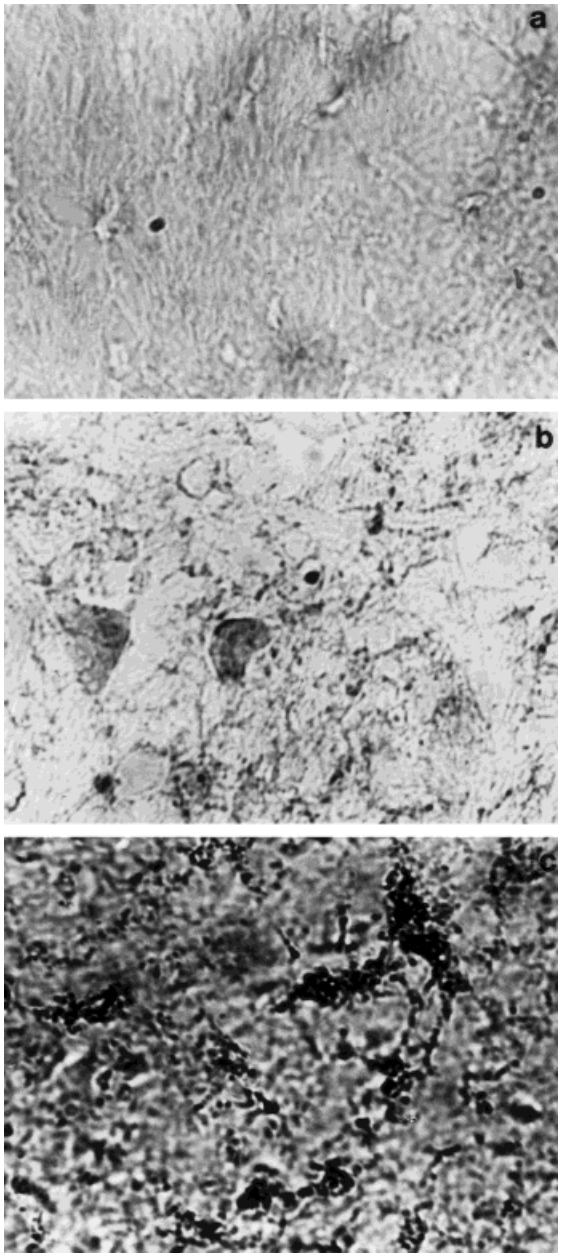

Fig. 4. Representative photomicrographs of IgG immunostaining staining in the medial geniculate nucleus. **a:** From a control rat. **b,c:** Sections from TD rats sacrificed after 10 days and at the loss of righting reflex stage respectively (all ×250). On day 10 of TD, IgG immunostaining is observed primarily in close proximity to blood vessels. By the loss of righting reflex stage, intense immunostaining extends to the surrounding parenchyma.

able brain regions including the inferior olive, medial thalamus, vestibular nuclei, and the inferior colliculus. Focal increases of IgG immunostaining were observed as early as 9 days into the TD protocol in two of six animals, and in the remainder after 10 days of TD. IgG immunostaining was initially confined to areas around small blood vessels. More widespread increases in IgG immunostaining were observed by day 13 (Fig. 4).

Figures 5, 6, and 7 compare IgG, ED1, GFAP immunostaining, and neuronal cell counts from the inferior olivary nucleus, medial geniculate nucleus, and medial dorsal nucleus of the thalamus, respectively. These specific nuclei were representative of all vulnerable brain nuclei assessed.

No increases of immunostaining above background levels were observed in any of the sections processed without primary antibodies. Similarly, no significant immunostaining for any of the antibodies tested was observed in non vulnerable regions such as the stria-

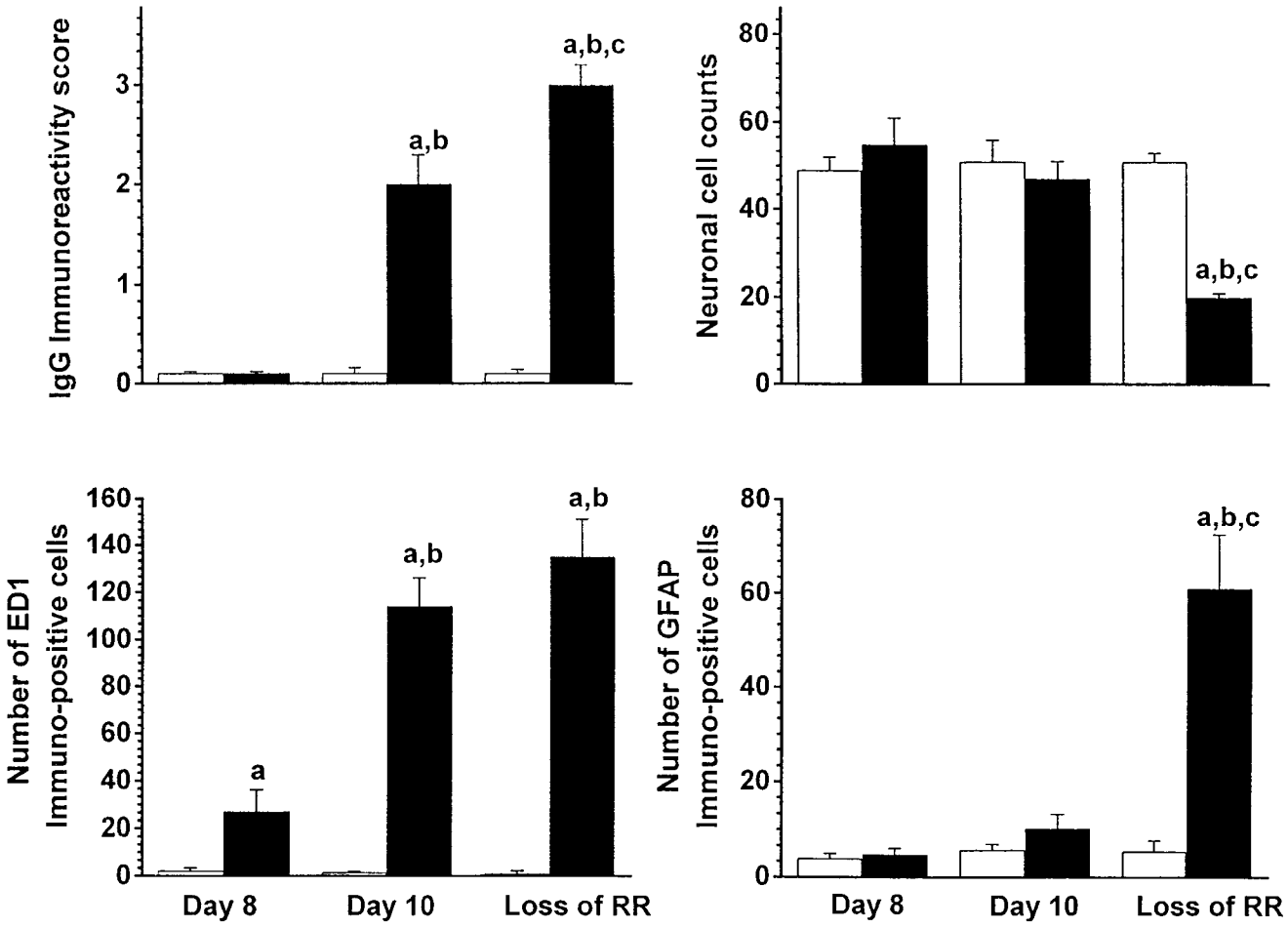

Fig. 5. Comparison of the timecourse of IgG, ED1, and GFAP immunostaining and neuronal cell counts from the medial geniculate nucleus of the thalamus of control and TD rats. Data represent mean ± SD of control animals (open bars, n = 4) and TD animals (closed bars, n = 6). **a:** Data significantly different from same day control values: **b:** Data significantly different from TD day 8 values. **c:** Data significantly different from TD day 10 values ($P < 0.05$). For neuronal cell counts, ED1, and GFAP immunostaining, two-way ANOVA was applied to the data. Kruskall-Wallis non parametric statistic was used for comparison of the IgG immunoreactivity scores at the various time points.

tum and frontal motor cortex of TD animals (data not shown).

DISCUSSION

The results of the present study reveal early, region-selective, increased ED1-immunostaining in specific thalamic nuclei including the periventricular nucleus, medial dorsal nucleus, and medial geniculate nucleus, as well as in the medial and lateral vestibular nucleus, inferior colliculus, and inferior olive regions of brain, which ultimately manifest significant neuronal loss in this experimental model of thiamine deficiency (Troncoso et al., 1981, Victor et al., 1989; Zhang et al., 1995; Todd and Butterworth, 1997a). Focal IgG immunostaining indicative of early loss of integrity of the blood–brain barrier was observed in these brain structures starting 2 days later (on day 10 of the treatment protocol) than the ED1 changes. These findings of increase IgG immunostaining confirm those of previous studies in pyrithiamine-induced TD (Calingasan et al., 1995, Harata and Iwasaki, 1995). Increases of GFAP-immunostaining were an even later event with significant changes occurring from day 11 of TD. These findings confirm and extend those of early histopathologic studies in which glial cell changes were reported to precede neuronal cell loss in experimental TD (Collins, 1967; Robertson et al., 1968; Tellez and Terry, 1968; Watanabe and Kanabe, 1978; Aikawa et al., 1984).

The ED1 antibody selectively labels a cytoplasmic antigen in microglia/macrophages (Dijkstra et al., 1985). Following neuronal injury, activated microglia and reactive (phagocytic) microglia express the ED1 antibody (Graeber et al., 1990). However, it was previously demonstrated in an experimental model of global ischemia that ED1-positive cells accumulate not only in areas of significant neuronal loss but also in areas in which no neuronal loss is initially apparent (Gehrmann et al., 1992). Results of the present study provide another example of this phenomenon. Furthermore, the present finding of increased ED1 immunostaining prior

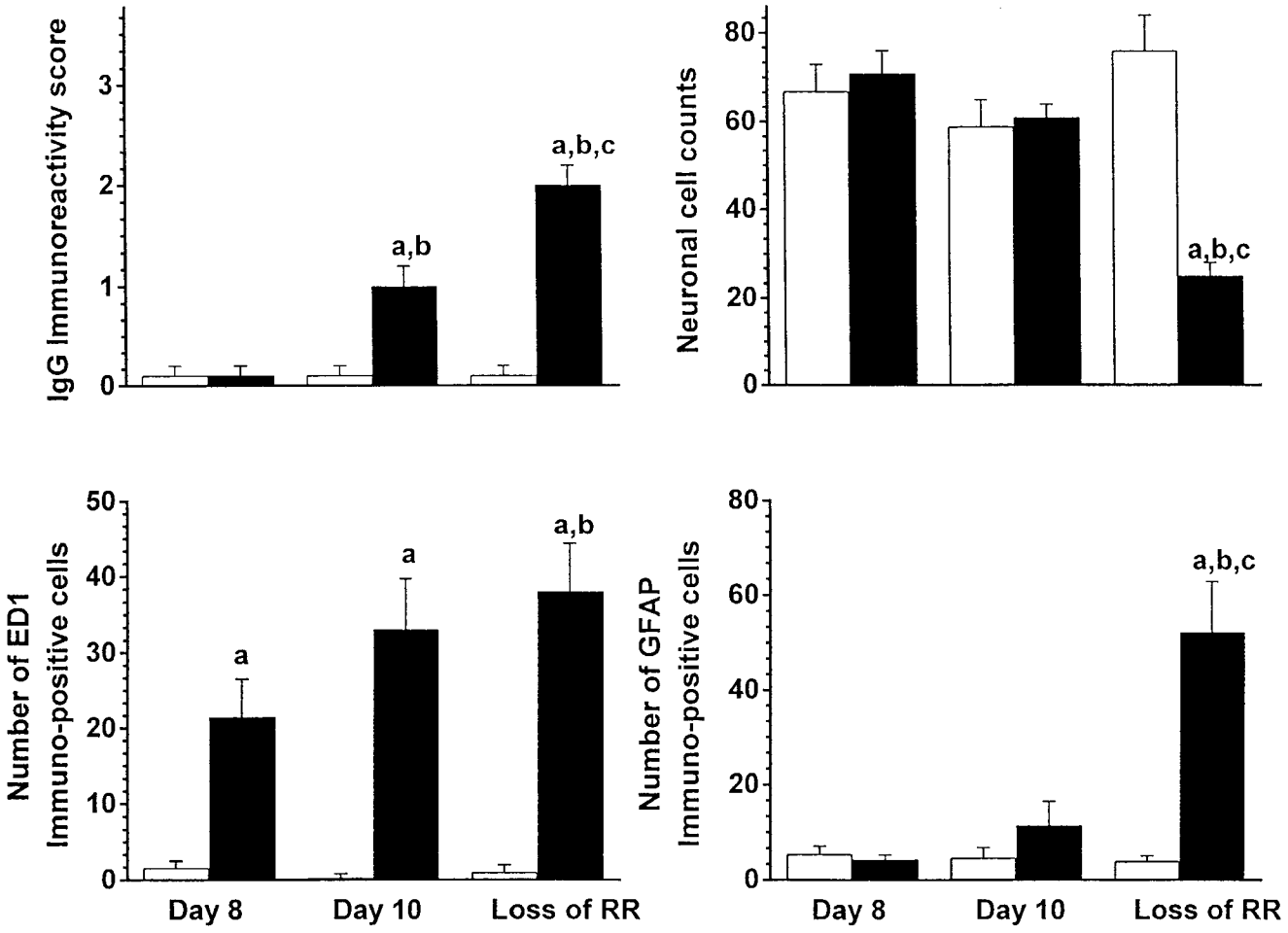

Fig. 6. Comparison of the timecourse of IgG, ED1, and GFAP immunostaining and cresyl violet staining from the medial dorsal nucleus of the thalamus of control and TD rats. Remainder of legend as for Figure 5.

to any evidence of blood–brain barrier breakdown suggests that early activation of resident microglia rather than infiltration of blood-borne macrophages is the initial glial change due to TD. Further studies to assess this intriguing possibility are therefore warranted.

Microglial activation occurs as a result of a well-established sequence of mechanisms involving cell proliferation and recruitment to the site of insult as well as by morphological, immunophenotypical, and functional modifications, regardless of the metabolic insult (Streit et al., 1988; Gehrmann et al., 1992, 1995; Dickson et al., 1993). Once activated, microglia release several mediator substances and cytotoxins including reactive oxygen intermediates (Gehrmann et al., 1992; Banati et al., 1993, 1994) and glutamate (Piani et al., 1991), both of which have been implicated in the pathogenesis of neuronal cell loss in experimental TD. Evidence for cerebral damage due to reactive oxygen species per se in experimental TD comes from reports of increased reactive oxygen species (Langlais et al., 1997) and of increased immunostaining for the free radical metabolizing enzyme superoxide dismutase (Todd and Butterworth, 1997b) in the brains of these animals. Moreover, microglia release large amounts of H_2O_2 (Flaris et al., 1993) and L-deprenyl, a monoamine oxidase B inhibitor known to reduce the enzymatic production of H_2O_2, is neuroprotective in experimental TD (Todd and Butterworth, 1998). Other reports provide evidence for increased concentrations of extracellular glutamate in vulnerable brain structures in this experimental model of TD (Hazell et al., 1993; Langlais and Zhang, 1993). Although it is likely that this increased glutamate release originates from depolarization of presynaptic nerve terminals, a microglial source could also be implicated.

The present findings of increased ED1 immunostaining prior to the occurrence of increased GFAP-immunoreactive cells supports previous findings in experimental global ischemia, where it was suggested that microglial activation could be causally related to the phenomenon of astrocytic proliferation (Gehrmann et al., 1995). It has been suggested that metabolically compromised neurons could initiate, by cell-to-cell signalling pathways, microglial activation as an initial cellular event in experimental cerebral ischemia (Gehrmann et al., 1992). Similar mechanisms could explain

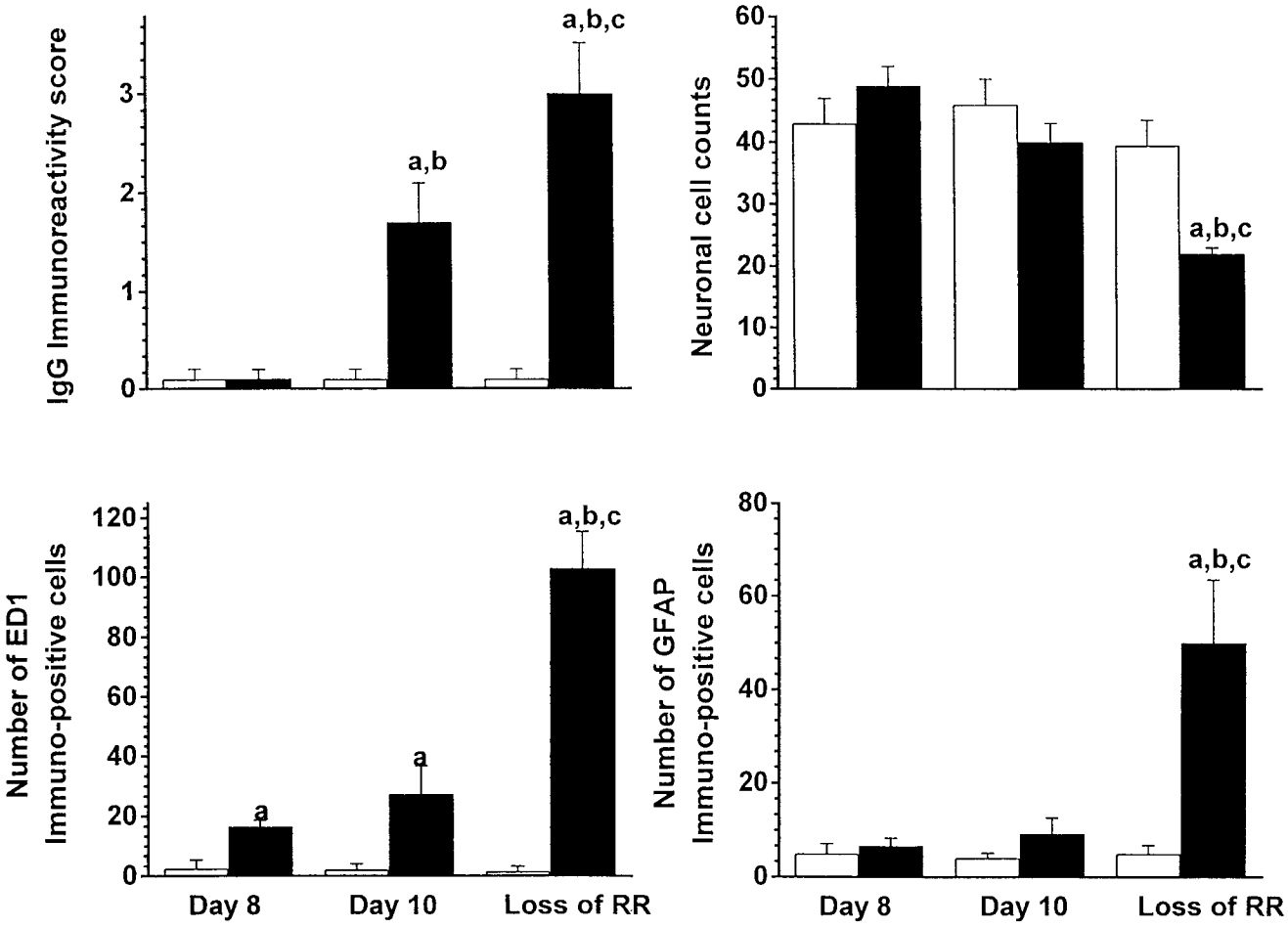

Fig. 7. Comparison of the timecourse of IgG, ED1, and GFAP immunostaining and cresyl violet staining from the inferior olivary nucleus of control and TD rats. Remainder of legend as for Figure 5.

the early increases of ED1 immunoreactivity observed in the present study.

The nature of the metabolic insult in pyrithiamine-induced TD is well established and consists of region-selective alterations of thiamine-dependent enzymes (Gibson et al., 1984; Butterworth et al., 1985, 1986; Giguere et al., 1987), lactate accumulation (Hakim, 1984), and reduced synthesis of ATP (Aikawa et al., 1984; McCandless, 1985). It is unlikely that the above metabolic changes are implicated in the triggering of early microglial activation as they typically occur later in the experimental paradigm (day 10 or later). Therefore, the results of the present study suggest that TD triggers an early and presently unknown injury leading to microglial activation. Future studies aimed at the investigation of the possible involvement of other microglial-derived cytotoxins including the cytokines interleukin-1 and interleukin-4 in the pathogenesis of neuronal cell loss in this experimental model of TD are presently underway.

In summary, the pyrithiamine model of TD in the rat recapitulates many of the cardinal neuropathologic (Troncoso et al., 1981) and biochemical (Heroux and Butterworth, 1992) features of Wernicke Encephalopathy (WE) in humans. It has therefore been extensively used as an experimental animal model for the study of pathophysiologic mechanisms responsible for neuronal cell death in this disorder. Mechanisms so far proposed include cellular energy failure (Hakim and Pappius, 1983), focal lactic acidosis, (Hakim, 1984), disruption of the blood–brain barrier (Calingasan et al., 1995; Harata and Iwasaki, 1996), and NMDA-mediated cytotoxicity (Hazell et al., 1993; Langlais and Zhang, 1995; Todd and Butterworth, 1997a). Results of the present study suggest that the initial cellular event due to TD involves microglial activation. Interestingly, pathological findings in human WE tissue reveal that in minimally affected cases, a proliferation of microglia precedes any signs of neuronal cell loss (Victor et al., 1989), further suggesting the possibility of early microglial involvement in the pathogenesis of selective neuronal cell death in this disorder.

REFERENCES

Aikawa HS, Watanabe IS, Furuse T, Iwasaki Y, Satoyoshi E, Sumi T, Moroji T. 1984. Low energy levels in thiamine-deficient encephalopathy. J Neuropathol Exp Neurol 43:276–287.

Banati RB, Gehrmann J, Schubert P, Kreutzberg GW. 1993. Cytotoxicity of microglia. Glia 7:111–118.

Banati RB, Schubert P, Rothe G, Gehrmann J, Rudolphi K, Valet G, Kreutzberg GW. 1994. Modulation of intracellular formation of reactive oxygen intermediates in peritoneal macrophages and microglia/brain macrophages by propentofylline. J Cereb Blood Flow Metab 14:145–149.

Butterworth RF, Giguere JF, Besnard AM. 1985. Activities of thiamine-dependent enzymes in two experimental models of thiamine-deficiency encephalopathy. 1. The pyruvate dehydrogenase complex. Neurochem Res 10:1417–1428.

Butterworth RF, Giguere JF, Besnard AM. 1986. Activities of thiamine-dependent enzymes in two experimental models of thiamine-deficiency encephalopathy. 2. α-Ketoglutarate dehydrogenase. Neurochem Res 11:567–577.

Calingasan NY, Baker H, Sheu K-FR, Gibson G. 1995. Blood-brain barrier abnormalities in vulnerable brain regions during thiamine deficiency. Exp Neurol 134:64–72.

Collins GH. 1967. Glial changes in the brain stem of thiamine-deficient rats. Am J Pathol 50:791–814.

Dickson DW, Lee SC, Mattiace LA, Yen SC, Brosnan C. 1993. Microglia and cytokines in neurological disease, with special reference to AIDS and Alzheimer's disease. Glia 7:75–83.

Dijkstra CD, Dopp EA, Joling P, Kraal G. 1985. The heterogeneity of mononuclear phagocytes in lymphoid organs: distinct macrophage subpopulations in the rat recognized by monoclonal antibodies ED1, ED2 and ED3. Immunology 54:589–599.

Flaris NA, Densmore TL, Molleston MC, Hickey WF. 1993. Characterization of microglia and macrophages in the central nervous system of rats: definition of the differential expression of molecules using standard and novel monoclonal antibodies in normal CNS and in for models of parenchymal reaction. Glia 7:34–40.

Gehrmann J, Bonnekoh P, Miyazawa T, Hossman K-A, Kreutzberg GW. 1992. Immunocytochemical study of an early microglia activation in ischemia. J Cereb Blood Flow Metab 12:257–269.

Gehrmann J, Matsumoto Y, Kreutzberg GW. 1995. Microglia: intrinsic immunoeffector cell of the brain. Brain Res Rev 20:269–287.

Gehrmann J, Kreutzberg GW. 1993. Monoclonal antibodies against macrophages/microglia: immunocytochemical studies of early microglial activation in experimental neuropathology. Clin Neuropathol 12:301–306.

Gibson GE, Kziezak-Reding H, Sheu K-FR, Mykytyn V, Blass JP. 1984. Correlation of enzymatic, metabolic and behavioral deficits in thiamine deficiency and its reversal. Neurochem Res 9:803–814.

Giguere JF, Butterworth RF. 1987. Activities of thiamine dependent enzymes in two experimental models of thiamine deficiency encephalopathy. 3. Transketolase. Neurochem Res 12:305–310.

Graeber MB, Streit WJ, Kiefer R, Schoen SW, Kreutzberg GW. 1990. New expression of myelomonocytic antigens by microglia and perivascular cells following lethal motor neuron injury. J Neuroimmunol 27:121–132.

Hakim AM. 1984. The induction and reversibility of cerebral acidosis in thiamine deficiency. Ann Neurol 16:673–679.

Hakim AM, Pappius HM. 1983. Sequence of metabolic, clinical and histological events in experimental thiamine deficiency. Ann Neurol 13:365–375.

Harata N, Iwasaki Y. 1995. Evidence for early blood-brain barrier breakdown in experimental thiamine deficiency in the mouse. Metab Brain Dis 10:159–174.

Harata N, Iwasaki Y. 1996. The blood-brain barrier and selective vulnerability in experimental thiamine-deficiency encephalopathy in the mouse. Metab Brain Dis 11:55–69.

Hazell AS, Butterworth RF, Hakim AM. 1993. Cerebral vulnerability is associated with selective increase in extracellular glutamate concentration in experimental thiamine deficiency. J Neurochem 61:1155–1158.

Heroux M, Butterworth RF. 1992. Animal models of the Wernicke-Korsakoff syndrome. In: Boulton A, Baker G and Butterworth RF, editors. Neuromethods. Vol. 22. Animal models of neurological disease. Humana Press, Totawa, Vol. II, pp 95–131.

Langlais PJ, Anderson G, Guo SX, Bondy SC. 1997. Increased cerebral free radical production during thiamine deficiency. Metab Brain Dis 12:137–143.

Langlais PJ, Zhang SX. 1993. Extracellular glutamate is increased in thalamus during thiamine deficiency-induced lesions and is blocked by MK801. J Neurochem 61:2175–2182.

McCandless DW. 1985. Thiamine deficiency and cerebral metabolism. In: Cerebral Energy Metabolism and Metabolic Encephalopathy. McCandless DW, ed. Plenum Press, New York. p 335–352.

Myers R, Manjil LG, Cullen BM, Price, GW, Frackowiak RSJ, Cremer JE. 1991. Macrophage and astrocyte populations in relation to [3H]PK 11195 binding in rat cerebral cortex following a local ischemic lesion. J Cereb Blood Flow Metab 11:314–322.

Paxinos G, Watson C. 1986. The rat brain in stereotoxic coordinates. San Diego, CA, Academic Press.

Piani D, Frei K, Do KO, Cuenod M, Fontana A. 1991. Murine brain macrophages induce NMDA receptor mediated neurotoxicity by secreting glutamate. Neurosci Lett 133:159–162.

Robertson DM, Wasan SM, Skinner DB. 1968. Ultrastructural features of early brain stem lesions of thiamine-deficient rats. Am J Pathol 52:1081–1087.

Streit WJ, Graeber MB, Kreutzberg GW. 1988. Functional plasticity of microglia: a review. Glia 1:301–307.

Tellez I, Terry RD. 1968. Fine structure of the early changes in the vestibular nuclei of the thiamine-deficient rat. Am J Pathol 52:777–794.

Todd KG, Butterworth RF. 1997a. Evaluation of the role of NMDA-mediated excitotoxicity in the selective neuronal loss in experimental Wernicke encephalopathy. Exp Neurol 149:130–138.

Todd KG, Butterworth RF. 1997b. Evidence that oxidative stress plays a role in neuronal cell death due to thiamine deficiency. J Neurochem 69:S136A.

Todd KG, Butterworth RF. 1998. Increased neuronal cell survival after L-deprenyl treatment in experimental thiamine deficiency. J Neurosci Res 52:240–246.

Troncoso JC, Johnston MV, Hess KM, Griffin JW, Price DL. 1981. Model of Wernicke's encephalopathy. Arch Neurol 38:350–354.

Victor M, Adams RD, Collins GH. 1989. The Wernicke-Korsakoff Syndrome 2nd Edition. Philadelphia: F.A. Davis Company.

Watanabe I, Kanabe S. 1978. Early edematous lesion of pyrithiamine induced acute thiamine deficient encephalopathy in the mouse. J Neuropathol Exp Neurol 36:401–413.

Zhang SX, Weilersbacher GS, Henderson SW, Corso T, Olney JW, Langlais PJ. 1995. Excitotoxic cytopathology, progression and reversibility of thiamine deficiency-induced diencephalic lesions. J Neuropathol Exp Neurol 54:255–267.